

Achieving Utility, Fairness, and Compactness via Tunable Information Bottleneck Measures

Adam Gronowski, William Paul, Fady Alajaji, Bahman Ghahsifard, and Philippe Burlina

Abstract—Designing machine learning algorithms that are accurate yet fair, not discriminating based on any sensitive attribute, is of paramount importance for society to accept AI for critical applications. In this article, we propose a novel fair representation learning method termed the Rényi Fair Information Bottleneck Method (RFIB) which incorporates constraints for utility, fairness, and compactness of representation, and apply it to image classification. A key attribute of our approach is that we consider – in contrast to most prior work – both demographic parity and equalized odds as fairness constraints, allowing for a more nuanced satisfaction of both criteria. Leveraging a variational approach, we show that our objectives yield a loss function involving classical Information Bottleneck (IB) measures and establish an upper bound in terms of the Rényi divergence of order α on the mutual information IB term measuring compactness between the input and its encoded embedding. Experimenting on three different image datasets (EyePACS, CelebA, and FairFace), we study the influence of the α parameter as well as two other tunable IB parameters on achieving utility/fairness trade-off goals, and show that the α parameter gives an additional degree of freedom that can be used to control the compactness of the representation. We evaluate the performance of our method using various utility, fairness, and compound utility/fairness metrics, showing that RFIB outperforms current state-of-the-art approaches.

Index Terms—Deep learning, fair representation learning, image classification, information bottleneck (IB), Rényi divergence.

I. INTRODUCTION

MACHINE learning algorithms are used for a variety of high stake applications such as loan approvals, police allocation, admission of students, and disease diagnosis. In spite of its vast benefits, the use of automated algorithms that are not designed to also address potential bias and fairly serve members of diverse groups can lead to harm and exacerbate social inequities. The problem of developing algorithms that are both accurate and *fair*, i.e., do not discriminate against individuals because of their gender, race, age, or other protected attributes, has now become paramount to the deployment

of production-grade AI systems that could be accepted and adopted by society as a whole.

Fair machine learning methods have been developed for multiple domains such as automated healthcare diagnostics and treatments delivery [2], natural language processing [3], and others [2], [4]–[6]. One way to create such fair machine learning methods is through learning *fair representations* that can be used with existing architectures. These representations would allow for making accurate predictions while ensuring fairness. However, this leads to the difficulty that developing fair representations may involve trade-offs and is further complicated by the existence of various metrics for measuring fairness outcomes, often tailored towards different applications and settings.

Our work entails the development of a fair representation learning method that addresses a number of trade-offs. Unlike most prior studies that tend to focus on satisfying a single type of fairness constraint, we consider here how to jointly address and balance two of the arguably most important definitions for fairness, *demographic parity* and *equalized odds*. We also examine different classical trade-offs between fairness and utility (commonly measured via accuracy). Trade-offs between utility and fairness arise as a result of interventions on models or data to make models more fair, which may yield decreased bias, but may also result in affecting utility. We study how these trade-offs are impacted by “compactness.” More specifically, we develop a variational approach taking into account different information-theoretic metrics that balance the above two constraints on fairness with utility and compactness. We also show how to analytically simplify the resulting loss function and relate it to the *Information Bottleneck (IB)* principle [7], and then exploit bounds to compute these metrics.

This work thus makes the following novel contributions:

- 1) We develop a novel variational method that balances a triplet of objectives, consisting of utility (accuracy), fairness (itself balancing two types of fairness constraints), and compression/compactness. Specifically, in contrast to prior work on fairness which narrowly uses either the demographic parity or equalized odds constraints, our loss includes both types of constraints. We relate analytically the resulting loss function to the classical IB method.
- 2) Operationally, we derive an upper bound on the mutual information between the data and its representation in terms of the Rényi divergence of order α . We study the effect of this added flexibility on achieving a balance between fairness and accuracy.
- 3) We compare, using various datasets such as CelebA, EyePACS, and FairFace, with methods of record that

This work was supported in part by the Natural Sciences and Engineering Research Council of Canada. (*Corresponding author: Adam Gronowski.*)

A preliminary version of part of this work was presented as [1] in the 2022 Canadian Workshop on Information Theory.

A. Gronowski and F. Alajaji are with the Department of Mathematics and Statistics, Queen’s University, Kingston, ON K7L 3N6, Canada (e-mail: adam.gronowski@queensu.ca; fa@queensu.ca).

W. Paul and P. Burlina are with the Johns Hopkins University Applied Physics Laboratory, Laurel, MD 20723 USA (e-mail: william.paul@jhuapl.edu; philippe.burlina@jhuapl.edu).

B. Ghahsifard is with the Electrical & Computer Engineering Department, University of California at Los Angeles, Los Angeles, CA 90095 USA (e-mail: ghahsifard@ucla.edu).

intervene on the model or methods that intervene on training data. We show that our method overall performs best. We establish these comparisons via a number of metrics that measure utility and fairness individually or in a combined metric, including two different types of fairness constraints.

The rest of the article is organized as follows. We present related work in Section II and derive a cost function for our method in Section III. In Section IV, we describe the details of our implementation, describe the metrics and datasets used, and present extensive experimental results. Finally, we conclude the article with Section V.

II. RELATED WORK

A. Fairness Approaches

We summarize existing work on fair machine learning in three categories. For a broad-strokes categorization of fairness approaches, one can think along the lines of *interventions* made either on: a) the model output, b) the training data, or c) the model itself. Each of these are motivated by different inductive biases.

1) *Interventions on Model Outputs Including Recalibration and Thresholding*: The inductive bias here is that irrespective of the cause of bias, fairness can be addressed at the output of the model. Some of these methods intervene on the model output via altering the decision threshold so that equal odds constraints are achieved, as in [8] by selecting an operating point where the receiver operating characteristic curves for different populations intersect (or variations on this approach). Alternatively, [9] uses re-calibration across subpopulations to debias models. While these methods are often effective – especially in case of debiasing models operating on categorical data – they have limitations in that they do not make more consequent changes on the data and the model itself to address the root causes of bias, as was argued also in [8]. This may especially be an issue for image/video applications and is the reason why an alternate path is pursued herein.

2) *Interventions on Data Including Generative Models and Style Transfer*: Such methods proceed from the inductive bias that interventions be carried on data, since data imbalance is a potential cause of biased models. Methods that modify the training data perform various operations, ranging from censoring sensitive information in the image domain to making it blind to protected factors, performing data augmentation, or using re-weighting of the data to achieve re-balancing either via data re-sampling or reweighting of the loss function. Data augmentation methods use generative models or style transfer/image translation. Notable approaches using generative models and based on generative adversarial networks (GANs) include [10]–[12]. In [13], image translation between protected populations was used to achieve normalized appearances. Translation and style transfer methods however have limitations in that they tend to collapse to using only a single style, a form of mode collapse, which may be an issue if data representative of a subpopulation entails “variations of styles,” such as in images. As will be discussed later, these methods are also related to interventions used for domain adaptation and

use cases of distributional shift and prior shift. Alternatively, [14] uses variational autoencoders for augmentation. Other examples of such generative methods for fairness include [15]. The methods in [12] use instead GANs along with a form of gradient descent in latent space to manipulate images and generate more data.

Generation of data using all of the above generative approaches has limitations as it may be hard to control the exact image markers that correspond to a specific protected factor without changing other markers (a problem known as *entanglement*). Also generation of images for canonical domains (faces, retinas, chest X-rays) tends to be relatively easily accomplished at present [16], but it may be more complicated for other domains. Generative methods may also yield artifacts in synthetic images, which could lead to a decrease in performance and in overall utility when debiasing without necessarily achieving significant gains in fairness. Aligned with these observations, it is suggested in [12] that for this reason model-altering fairness methods may outperform data-altering methods via generative models. These limitations motivate our approach, which falls in the category of interventions to the model itself, described next.

3) *Interventions on Models via Adversarial and Variational Approaches*: Such methods are grounded on the inductive bias that dependence of the prediction on protected factors is a cause of lack of fair predictions; as a result, these methods generally aim to remedy this dependence at the encoding of the data, rendering them blind to protected factors.

Studies such as [17] and [18] use an adversarial network to penalize the prediction network if it could predict a protected factor. Other works employ adversarial representation learning to remove protected factor information from latent representations, including [19]–[23]. Applications using this principle include [24] which uses adversarial learning to develop fair models of cardiovascular disease risk, while [25] explores the statistical properties of fair representation learning and [26] applies an adversarial approach for continuous features. Similar to our work, [27] employs an information-theoretic approach to learn fair representations. But in contrast to the above methods that are based on an adversarial approach, our method does not use adversarial training.

In addition to the above methods, there also exist non-adversarial methods that modify the model via incorporation of multiple constraints in a variational setting. Many of these are closely related to the IB method that we discuss next.

B. Information Bottleneck Methods

The IB method, originally proposed by Tishby *et al.* [7], is a method that seeks to develop representations that are both compact and expressive by minimizing and maximizing two mutual information terms. Alemi *et al.* first developed a variational approximation of the IB method by parameterizing it using neural networks and this was followed by multiple variations such as the nonlinear information bottleneck [28] and conditional entropy bottleneck [29]. Many recent generalizations of the IB method have been developed including [30]–[34] while [35], [36] investigated its connections to deep learning theory and privacy applications.

Techniques related to the information bottleneck have been used for fair representation learning. First proposed by [4], fair representation learning consists of mapping input data to an intermediate representation that remains informative but discards unwanted information that could reveal the protected sensitive factors. This is related to the IB problem and several works have explored the connection between the two, such as Ghassami *et al.* [37] and Rodríguez-Gálvez *et al.* [38] where fair representations are acquired through the minimization and maximization of various mutual information terms.

Our work is closest to [38] but we depart from it in several important ways, including through the use of a more general loss formulation, satisfying broader constraints of fairness, classifying images rather than focusing solely on tabular data, and entailing the use of Rényi divergence. To our knowledge we are the first to use Rényi divergence for fair representation learning but there have been several recent works based on Rényi information measures and its variants. These include an IB problem under a Rényi entropy complexity constraint [34], bounding the generalization error in learning algorithms [39], Rényi divergence variational inference [40], Rényi differential privacy [41] and the analysis and development of deep generative adversarial networks [42]–[45]. In addition, Baharlouei *et al.* [46] developed a fair representation method but one based on Rényi correlation rather than divergence.

C. Connections to Other Work

Fairness is related to the problem of domain adaptation (DA) [47]–[50] that consists of training a neural network on a source dataset to obtain good accuracy on a target dataset that is different from the source. This is especially true for the case of a severe data imbalance that we consider in this work where training data is completely missing for a protected subgroup. In this case, achieving fairness is similar to the DA problem of improving performance on a complete target dataset that includes all groups after training on an incomplete source dataset.

Our work is also related to group distributionally robust optimization (GDRO) methods [51], [52] that address the problem of performance disparity among different subgroups by minimizing the worst-case loss among different subgroups. Reducing these accuracy differences among subgroups is something our method also addresses, but while this is the sole objective for GDRO methods, we consider this problem in relation to multiple other fairness criteria.

There are some other work that investigated finding a balance between accuracy and fairness such as Zhang *et al.* [53]. However, they achieved this objective by finding early stopping criteria rather than through a fair representation pre-processing method like we use here; also, unlike our method, finding a balance between multiple fairness constraints is not investigated.

Finally, there are hybrid methods, such as the one proposed by Paul *et al.* in [12], that use a combination of the previously discussed techniques of interventions on data, model, or output. However, such techniques are quite limited in scope compared to the more varied objectives considered here which involve jointly achieving utility, fairness, and compactness.

III. METHODS

We take an information-theoretic approach to fairness. We represent input data as a random variable $X \in \mathcal{X}$ and sensitive information as a random variable $S \in \mathcal{S}$. Our goal is to use the data X to predict a target $Y \in \mathcal{Y}$ but in a way that is uninfluenced by the sensitive information S . To reach this objective, we adopt a variational approach, which we call *Rényi Fair Information Bottleneck* (RFIB), to encode the data into a new representation $Z \in \mathcal{Z}$. The representation can then be used with existing deep learning model architectures to draw inferences about Y . In light of our model, we assume that the Markov chain $(Y, S) \rightarrow X \rightarrow Z$ holds. To simplify notation, we assume in this section that all random variables are discrete, though a similar derivation holds for a mix of continuous and discrete random variables.

A. Fairness Defined

Among the three principal definitions of fairness – *demographic parity*, *equalized odds*, and *equality of opportunity* – we focus on addressing both demographic parity and equalized odds since a) equalized odds is related to (but a stronger constraint than) equality of opportunity, and b) demographic parity, also called statistical parity, is an altogether different type of constraint compared to the former two constraints in that the requirement of independence does not involve the actual target label value.

For demographic parity, the goal is for the model’s prediction \hat{Y} to be independent of the sensitive variable S , i.e.,

$$P(\hat{Y} = \hat{y}) = P(\hat{Y} = \hat{y} \mid S = s) \quad (1)$$

for all s, \hat{y} , while for equalized odds the goal is to achieve this independence by conditioning on the actual target Y , i.e.,

$$P(\hat{Y} = \hat{y} \mid Y = y) = P(\hat{Y} = \hat{y} \mid S = s, Y = y) \quad (2)$$

for all s, \hat{y}, y .

B. Lagrangian Formulation

To encourage equalized odds, we minimize $I(Z; S|Y)$; i.e., we minimize the average amount of information that Z has about S given Y . To both obtain good classification accuracy and help promote demographic parity, we maximize $I(Z; Y|S)$. Maximizing mutual information between Z and Y ensures the representation will be expressive about its target while the conditioning on S ensures that Z does not keep information shared by S , encouraging demographic parity.

In addition, we minimize $I(Z; X|S, Y)$, a compression term similar to one from the IB problem [54]. This minimization further encourages Z to discard information irrelevant for drawing predictions about Y , hence improving generalization capability and reducing the risk of keeping nuisances. Finally, we maximize the utility term $I(Z; Y)$; this optimization, similar to the IB problem, solely ensures the representation is maximally expressive of the target Y .

Combining these terms leads to a Lagrangian, \mathcal{L} , that we seek to minimize over the encoding conditional distribution $P_{Z|X}$. The Lagrangian is given by

$$\mathcal{L} = I(Z; S|Y) + I(Z; X|S, Y) - \lambda_1 I(Z; Y) - \lambda_2 I(Z; Y|S), \quad (3)$$

where λ_1 and λ_2 are hyperparameters. Developing this Lagrangian, we have that

$$\begin{aligned} \mathcal{L} &= H(Z|Y) - H(Z|S, Y) + H(Z|S, Y) \\ &\quad - H(Z|X, S, Y) - \lambda_1 I(Z; Y) - \lambda_2 I(Z; Y|S) \\ &= H(Z|Y) - H(Z|X) - \lambda_1 I(Z; Y) - \lambda_2 I(Z; Y|S) \\ &= H(X) - H(Z, X) - [H(Y) - H(Z, Y)] \\ &\quad - \lambda_1 I(Z; Y) - \lambda_2 I(Z; Y|S) \\ &= I(Z; X) - I(Z; Y) - \lambda_1 I(Z; Y) - \lambda_2 I(Z; Y|S) \\ &= I(Z; X) - (\lambda_1 + 1)I(Z; Y) - \lambda_2 I(Z; Y|S), \end{aligned} \quad (4)$$

where $H(\cdot)$ denotes entropy, and the second equality follows from the Markov chain assumption $(Y, S) \rightarrow X \rightarrow Z$. Hence, we have shown that the Lagrangian \mathcal{L} admits a simpler equivalent expression given by

$$\mathcal{L} = I(Z; X) - \beta_1 I(Z; Y) - \beta_2 I(Z; Y|S), \quad (5)$$

where $\beta_1 = \lambda_1 + 1 \geq 0$ and $\beta_2 = \lambda_2 \geq 0$. This simpler Lagrangian is easier to compute while exactly maintaining the properties of the original one. It also reveals a direct relation of the original Lagrangian with the first two terms being exactly equivalent to the ‘‘classical IB’’ formulation. The two hyperparameters β_1 and β_2 control trade-offs between accuracy (or ‘‘utility’’) and fairness, with higher β values corresponding to a higher priority on accuracy and lower β values giving more influence to the compression term $I(Z; X)$ that discards unwanted information, potentially improving fairness at the expense of accuracy. As $I(Z; Y)$ is partially derived from the $I(Z; S|Y)$ term designed to improve equalized odds, using a higher β_1 over β_2 should give more priority to improving equalized odds, whereas a higher β_2 should result in improved demographic parity. This allows for more nuanced outcomes compared to other methods that focus rigidly on a single fairness metric. It is also possibly an interesting tool for policy makers to translate those more balanced and nuanced versions of fairness into an ‘‘engineered system.’’

C. Variational Bounds

We use a variational approach to develop bounds on the three terms in the Lagrangian in (5), finding lower bounds for the terms to be maximized and an upper bound for the term to be minimized. The Markov chain property $(Y, S) \rightarrow X \rightarrow Z$ results in the joint distribution P_{SYXZ} factoring as $P_{SYX}P_{Z|X}$.

The distribution $P_{Z|X}$ is a parametric stochastic encoder to be designed while all other distributions are fully determined by the joint data distribution $P_{S,X,Y}$, the encoder, and the Markov chain constraint. To simplify notation, we simply write $P_{Z|X}$ rather than including the parameter $P_{Z|X,\theta}$, with θ denoting network weights. Computing the mutual information terms requires the usually intractable distributions $P_{Y|S,Z}$,

$P_{Y|Z}$, and P_Z ; we thus replace them with variational approximations $Q_{Y|S,Z}$, $Q_{Y|Z}$ and Q_Z , respectively. We next derive an upper bound for $I(Z; X)$ with the novel use of Rényi divergence:

$$\begin{aligned} I(Z; X) &= \sum_{(z,x) \in \mathcal{Z} \times \mathcal{X}} P_{Z,X}(z, x) \log \frac{P_{Z|X}(z|x)}{P_Z(z)} \\ &= \sum_{(z,x) \in \mathcal{Z} \times \mathcal{X}} P_{Z,X}(z, x) \log P_{Z|X}(z|x) \\ &\quad - D_{KL}(P_Z \| Q_Z) - \sum_{z \in \mathcal{Z}} P_Z(z) \log Q_Z(z) \\ &\leq \sum_{(z,x) \in \mathcal{Z} \times \mathcal{X}} P_{Z,X}(z, x) \log \frac{P_{Z|X}(z|x)}{Q_Z(z)} \\ &= \mathbb{E}_{P_X} D_{KL}(P_{Z|X} \| Q_Z) \\ &\leq \mathbb{E}_{P_X} D_\alpha(P_{Z|X} \| Q_Z), \end{aligned} \quad (6)$$

for $\alpha > 1$. The first inequality follows from the non-negativity of Kullback-Leibler (KL) divergence, similar to [27], [38], [54]. For the final step, we take the Rényi divergence $D_\alpha(\cdot \| \cdot)$ of order α (e.g., see [55]), rather than the KL divergence as typically done in the literature, where

$$D_\alpha(P \| Q) = \frac{1}{\alpha - 1} \log \left(\sum_{x \in \mathcal{X}} P(x)^\alpha Q(x)^{1-\alpha} \right) \quad (7)$$

for $\alpha > 0$, $\alpha \neq 1$ and distributions P and Q with common support \mathcal{X} .¹ Using Rényi divergence gives an extra degree of freedom and allows more control over the compression term $I(X; Z)$. As the Rényi divergence is non-decreasing with α , a higher α will more strongly force the distribution $P_{Z|X}$ closer to Q_Z , resulting in more compression.

The upper bound in (6) holds for $\alpha > 1$ since D_α is non-decreasing in α and $\lim_{\alpha \rightarrow 1} D_\alpha(P \| Q) = D_{KL}(P \| Q)$.² When $\alpha < 1$, then $\mathbb{E}_{P_X} D_\alpha(P_{Z|X} \| Q_Z)$ is no longer an upper bound on $I(Z; X)$; but it can be considered as a potentially useful approximation that is tunable by varying α .

We can similarly leverage the non-negativity of KL divergence to get lower bounds on $I(Z; Y)$ and $I(Z; Y|S)$:

$$I(Z; Y) \geq \mathbb{E}_{P_{Y,Z}} [\log Q_{Y|Z}(Y|Z)] + H(Y), \quad (8)$$

$$I(Z; Y|S) \geq \mathbb{E}_{P_{S,Y,Z}} [\log Q_{Y|S,Z}(Y|S, Z)] + H(Y|S). \quad (9)$$

As the entropy $H(Y)$ and conditional entropy $H(Y|S)$ of the labels do not depend on the parameterization they can be ignored for the optimization.

D. Computing the Bounds

To compute the bounds in practice we use the reparameterization trick [56]. Modeling $P_{Z|X}$ as a density, we let $P_{Z|X} dZ = P_E dE$, where E is a random variable and $Z = f(X, E)$ is a deterministic function, allowing us to backpropagate gradients

¹If P and Q are probability density functions, then $D_\alpha(P \| Q) = \frac{1}{\alpha - 1} \log \left(\int_{\mathcal{X}} P(x)^\alpha Q(x)^{1-\alpha} dx \right)$.

²For simplicity and by the continuity property of D_α in α , we define its extended orders at $\alpha = 1$ and $\alpha = 0$ [55] as $D_1(P \| Q) := D_{KL}(P \| Q)$ and $D_0(P \| Q) := \lim_{\alpha \rightarrow 0} D_\alpha(P \| Q) = -\log Q(x : P(x) > 0)$, which is equal to 0 when P and Q share a common support.

and optimize the parameter via gradient descent. We use the data's empirical densities to estimate $P_{X,S}$ and $P_{X,Y,S}$.

Considering a batch $D = \{x_i, s_i, y_i\}_{i=1}^N$ this finally leads to the following RFIB cost function to minimize:

$$J_{\text{RFIB}} = \frac{1}{N} \sum_{i=1}^N \left[D_\alpha(P_{Z|X=x_i} \| Q_Z) - \beta_1 \mathbb{E}_E [\log(Q_{Y|Z}(y_i | f(x_i, E)))] - \beta_2 \mathbb{E}_E [\log(Q_{Y|S,Z}(y_i | s_i, f(x_i, E)))] \right], \quad (10)$$

where we estimate the expectation over E using a single Monte Carlo sample.

We note that depending on the choice of α , β_1 , and β_2 , from our method we can recover both the *IB* [54] and *conditional fairness bottleneck* (CFB) [38] schemes to which we compare our results. Letting $\alpha = 1$ and $\beta_2 = 0$ corresponds to IB, while setting $\alpha = 1$ and $\beta_1 = 0$ corresponds to CFB.

E. Derivation of $D_\alpha(P_{Z|X} \| Q_Z)$ for Gaussians

Here we calculate the Rényi divergence term of our cost function when $P_{Z|X}$ and Q_Z are multivariate Gaussian distributions with $P_{Z|X}$ having a diagonal covariance structure while Q_Z being a spherical Gaussian. More specifically, we let

$$P_{Z|X} = \mathcal{N}(Z | \mu_{\text{enc}}(X), \text{diag}(\sigma_{\text{enc}}^2(X))) \quad \text{and} \\ Q_Z = \mathcal{N}(Z | \underline{0}, \gamma^2 I_d),$$

where μ_{enc} and σ_{enc}^2 are d -dimensional mean and variance vectors (that depend on X), $\text{diag}(\sigma_{\text{enc}}^2(X))$ is a $d \times d$ diagonal matrix with the entries of σ_{enc}^2 on the diagonal, $\underline{0}$ is the all-zero vector of size d , γ is a positive scalar, and I_d is the d -dimensional identity matrix. For simplicity of notation, in the rest of the article we write $\mu_{\text{enc}}(X)$ as μ_{enc} and $\text{diag}(\sigma_{\text{enc}}^2(X))$ as $\sigma_{\text{enc}}^2 I_d$.

Starting with the closed-form expression of the Rényi divergence of order α ($\alpha > 0$, $\alpha \neq 1$) derived in [57], [58], we have

$$D_\alpha(P_{Z|X} \| Q_Z) = \frac{\alpha}{2} (\mu'_{\text{enc}} [(\Sigma_\alpha)^*]^{-1} \mu_{\text{enc}}) - \frac{1}{2(\alpha-1)} \ln \frac{|(\Sigma_\alpha)^*|}{|\sigma_{\text{enc}}^2 I_d|^{1-\alpha} |\gamma^2 I_d|^\alpha} \quad (11)$$

where μ'_{enc} is the transpose of μ_{enc} ,

$$(\Sigma_\alpha)^* = \alpha \gamma^2 I_d + (1-\alpha) \sigma_{\text{enc}}^2 I_d,$$

and $\alpha[\sigma_{\text{enc}}^2 I_d]^{-1} + (1-\alpha)[\gamma^2 I_d]^{-1}$ is positive definite. Then

$$\frac{\alpha}{2} (\mu'_{\text{enc}} [(\Sigma_\alpha)^*]^{-1} \mu_{\text{enc}}) = \frac{\alpha}{2} \sum_{i=1}^d \frac{\mu_i^2}{\alpha \gamma^2 + (1-\alpha) \sigma_i^2}, \quad (12)$$

where μ_i and σ_i are the i th components of μ_{enc} and σ_{enc} and

$$\frac{1}{2(\alpha-1)} \ln \frac{|(\Sigma_\alpha)^*|}{|\sigma_{\text{enc}}^2 I_d|^{1-\alpha} |\gamma^2 I_d|^\alpha}$$

$$= \frac{1}{2(\alpha-1)} \ln \frac{\begin{vmatrix} \alpha \gamma^2 + (1-\alpha) \sigma_1^2 & \cdots & 0 \\ \vdots & \ddots & \vdots \\ 0 & \cdots & \alpha \gamma^2 + (1-\alpha) \sigma_d^2 \end{vmatrix}}{\begin{vmatrix} \sigma_1^2 & \cdots & 0 \\ \vdots & \ddots & \vdots \\ 0 & \cdots & \sigma_d^2 \end{vmatrix}^{1-\alpha} \begin{vmatrix} \gamma^2 & \cdots & 0 \\ \vdots & \ddots & \vdots \\ 0 & \cdots & \gamma^2 \end{vmatrix}^\alpha} \\ = \frac{1}{2(\alpha-1)} \ln \frac{\prod_{i=1}^d [\alpha \gamma^2 + (1-\alpha) \sigma_i^2]}{(\prod_{i=1}^d \sigma_i^2)^{1-\alpha} (\prod_{i=1}^d \gamma^2)^\alpha} \\ = \frac{1}{2(\alpha-1)} \sum_{i=1}^d \ln \frac{\alpha \gamma^2 + (1-\alpha) \sigma_i^2}{\sigma_i^{2(1-\alpha)} \gamma^{2\alpha}}, \quad (13)$$

yielding that

$$D_\alpha(P_{Z|X} \| Q_Z) = \frac{\alpha}{2} \sum_{i=1}^d \frac{\mu_i^2}{\alpha \gamma^2 + (1-\alpha) \sigma_i^2} - \frac{1}{2(\alpha-1)} \sum_{i=1}^d \ln \frac{\alpha \gamma^2 + (1-\alpha) \sigma_i^2}{\sigma_i^{2(1-\alpha)} \gamma^{2\alpha}}. \quad (14)$$

Since we require the matrix $\alpha[\sigma_{\text{enc}}^2 I_d]^{-1} + (1-\alpha)[\gamma^2 I_d]^{-1}$ to be positive definite, the above Rényi divergence expression is valid for

$$\alpha \gamma^2 + (1-\alpha) \sigma_i^2 > 0, \quad i = 1, \dots, d,$$

or equivalently (recalling that $\alpha > 0$, $\alpha \neq 1$) for

$$0 < \alpha < 1, \sigma_i^2 > 0, \quad i = 1, \dots, d, \\ \alpha > 1, \sigma_i^2 < \frac{\alpha \gamma^2}{\alpha - 1}, \quad i = 1, \dots, d. \quad (15)$$

We finish this section with a remark.

Remark (Limit as $\alpha \rightarrow 1$): Taking the limit of the Rényi divergence as $\alpha \rightarrow 1$ we recover, as expected, the KL divergence expression between Gaussians:

$$\lim_{\alpha \rightarrow 1} D_\alpha(P_{Z|X} \| Q_Z) \\ = \lim_{\alpha \rightarrow 1} \left[\frac{\alpha}{2} \sum_{i=1}^d \frac{\mu_i^2}{\alpha \gamma^2 + (1-\alpha) \sigma_i^2} - \frac{1}{2(\alpha-1)} \sum_{i=1}^d \ln \frac{\alpha \gamma^2 + (1-\alpha) \sigma_i^2}{\sigma_i^{2(1-\alpha)} \gamma^{2\alpha}} \right] \\ = \frac{1}{2} \sum_{i=1}^d \frac{\mu_i^2}{\gamma^2} - \lim_{\alpha \rightarrow 1} \frac{1}{2} \left[\sum_{i=1}^d \frac{\gamma^2 - \sigma_i^2}{\alpha \gamma^2 + (1-\alpha) \sigma_i^2} + 2 \ln \sigma_i - \ln \gamma^2 \right] \\ = -\frac{1}{2} \sum_{i=1}^d \left[\ln \sigma_i^2 - \ln \gamma^2 + 1 - \frac{\sigma_i^2}{\gamma^2} - \frac{\mu_i^2}{\gamma^2} \right] \\ = D_{KL}(P_{Z|X} \| Q_Z). \quad (16)$$

IV. EXPERIMENTS

We conduct experiments on three different image datasets: CelebA, FairFace, and EyePACS. In this section, we detail the implementation steps of our method, describe the metrics and the datasets we used, and explain how the experiments were performed and present results. We also present a uniform manifold approximation and projection (UMAP) clustering analysis that visualizes the effects of the hyper-parameter α .

A. Additional Implementation Details

For all experiments, we use an isotropic Gaussian distribution for the encoder with mean and variance learned by a neural network, $P_{Z|X} = \mathcal{N}(Z|\mu_{\text{enc}}, \sigma_{\text{enc}}^2 I_d)$, using the same notation as described in Section III-E. Leveraging the reparameterization trick, we compute our representation Z as $Z = \mu_{\text{enc}} + \sigma_{\text{enc}} \odot E$, where \odot is the element-wise product and $E \sim \mathcal{N}(0, I_d)$.

We model the approximation of the representation's marginal as a d -dimensional spherical Gaussian, $Q_Z = \mathcal{N}(Z|0, \gamma^2 I_d)$ and calculate the Rényi divergence in (10) between the multivariate Gaussians $P_{Z|X}$ and Q_Z using (14). For all experiments, we use a value of $\gamma = 1$. For $\alpha < 1$, by (15) there is no restriction on the values of σ_{enc}^2 so we let them be any positive number, while for $\alpha > 1$ we add an additional sigmoid function to the encoder to limit outputs such that all values of σ_{enc}^2 are < 1 . Finally, as we only use binary values for Y , we model $Q_{Y|Z}$ with Bernoulli distributions, $Q_{Y|Z} = \text{Bernoulli}(Y; f(Z))$ and $Q_{Y|Z,S} = \text{Bernoulli}(Y; g(Z, S))$ where f and g are auxiliary fully connected networks.

The encoder network $P_{Z|X}$ is a ResNet50 [59] classifier pretrained on ImageNet with the final linear layer replaced by two randomly initialized layers with output dimension d equal to the dimension of the representation. The two decoder networks f and g are each two fully connected layers with 100 units and a Sigmoid layer.

After creating the representation Z , we use a logistic regression classifier with default settings to predict Y from Z . We evaluate accuracy and fairness on these predictions. Fig. 1 shows the architecture of our model.

We preprocess images by taking a 128 by 128 pixel center crop of the 218 by 178 pixel CelebA images, and a 256 pixel by 256 pixel center crop of EyePACS images. For FairFace we use the full 224 pixel by 224 pixel images. We then split the training data into a training set and validation set, using 20% of the data for validation, and use the validation set for early stopping. We train for up to 20 epochs, with early stopping triggering when there is no decrease in validation loss for 5 epochs, using a `min_delta` value of 0.

For all experiments, we train using PyTorch on a NVIDIA GP100 GPU. We use $d = 32$ as the dimension of our representation Z , a batch size of 64, and the Adam optimizer with a learning rate of 0.001. For most experiments, we tune hyperparameters by varying α linearly from 0 to 1, with $\alpha = 0$ signifying

and with $\alpha = 1$ corresponding to $D_\alpha(P_{Z|X}||Q_Z)$ being given by the KL divergence $D_{KL}(P_{Z|X}||Q_Z)$ (see Footnote 2), and by varying β_1 and β_2 linearly from 1 to 50. We also perform some additional experiments with α values > 1 .

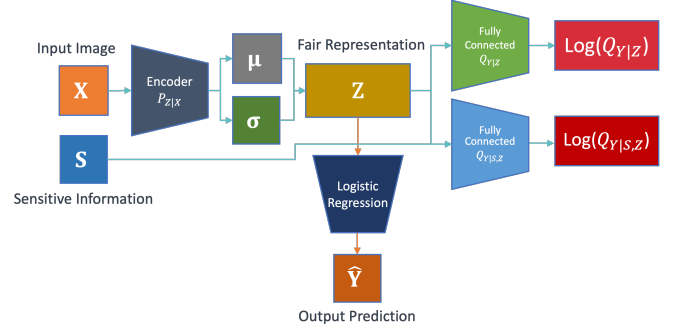


Fig. 1. Architecture of the model. The input image X is given to the encoder $P_{Z|X}$ that generates the mean μ and standard deviation σ for the distribution of the fair representation Z , $\mathcal{N}(Z|\mu_{\text{enc}}, \sigma_{\text{enc}}^2 I_d)$. Z is then given to two fully connected networks, one of which is also given the sensitive information S . After training, Z can be used as input to other existing architectures for fair prediction. For our experiments, we use logistic regression to predict Y from Z .

B. Metrics

We use the following metrics to evaluate how well the model performs:

- 1) *Measure of Utility*: We use the overall classification accuracy (later denoted *acc*).
- 2) *Measures of Fairness*: We measure this in multiple ways:
 - a) using the gap in accuracy (denoted acc_{gap}) between favored and protected subpopulations;
 - b) reporting the minimum accuracy across subpopulations (denoted as acc_{min}), which is based on the Rawlsian principle of achieving fairness by maximizing acc_{min} [60];
 - c) measuring the adherence to demographic parity via its gap dp_{gap} , following [38];
 - d) measuring the adherence using equalized odds via its gap $eqodds_{\text{gap}}$.

The latter two metrics are, respectively, given by:

$$dp_{\text{gap}} = |P(\hat{Y} = 1|S = 0) - P(\hat{Y} = 1|S = 1)| \quad (17)$$

and

$$eqodds_{\text{gap}} = \max_{y \in \{0,1\}} |P(\hat{Y} = 1|S = 0, Y = y) - P(\hat{Y} = 1|S = 1, Y = y)|. \quad (18)$$

3) *Joint Utility-Fairness Measure*: Echoing and comparing with the work in [12], we use a single metric that jointly captures utility and fairness, the Conjunctive Accuracy Improvement (CAI_λ) measure:

$$CAI_\lambda = \lambda(acc_{\text{gap}}^b - acc_{\text{gap}}^d) + (1 - \lambda)(acc^d - acc^b) \quad (19)$$

where $0 \leq \lambda \leq 1$, and acc^b and acc^d are the accuracy for baseline and debiased algorithms, respectively, while acc_{gap}^b and acc_{gap}^d are gap in accuracy for the baseline and debiased

$$D_0(P_{Z|X}||Q_Z) = -\log Q_Z(z : P_{Z|X}(z) > 0) = 0$$

algorithms. In practice, one can use $\lambda = 0.5$ for an equal balance between utility and fairness or a higher value such as $\lambda = 0.75$ to emphasize fairness.

C. Data

The datasets we use (sample images shown in Fig. 2) include the following:

1) *CelebA*: The CelebA dataset [61] contains 202,599 celebrity faces that each have 40 binary attributes. We use age as our prediction target Y and are interested in skin tone as the sensitive attribute S . As this is not included in the dataset we instead use the Individual Topology Angle (ITA) [62] as a proxy, which was found to correlate with the Melanin Index, frequently used in dermatology to classify human skin on the Fitzpatrick scale. As in [12], [63], we compute ITA via

$$\text{ITA} = \frac{180}{\pi} \arctan\left(\frac{L - 50}{b}\right), \quad (20)$$

where L is luminescence and b is yellowness in CIE-Lab space. We then binarize ITA where an ITA of ≤ 28 is taken to mean dark skin, matching category thresholds used in [12], [64].

2) *FairFace*: The FairFace dataset [65] consists of 108,501 face images labeled with race, gender, and age. We consider age as the target Y and race as sensitive information S . The dataset contains several different categories for race and age and we binarize them into Black and non-Black for race and ≥ 30 years old and < 30 years old for age.

3) *EyePACS*: The EyePACS dataset [66] is sourced from the Kaggle Diabetic Retinopathy challenge. It consists of 88,692 retinal fundus images of individuals potentially suffering from diabetic retinopathy (DR), an eye disease associated with diabetes that is one of the leading causes of visual impairment worldwide. The dataset contains 5 categories of images based on the severity of the disease, with 0 being completely healthy and 4 being the most severe form of the disease. Similar to [12], we binarize this label into our prediction target Y , with $Y = 1$ corresponding to categories 2-4, considered a positive, referable case for DR and $Y = 0$ corresponding to categories 0-1, considered healthy.

In our experiments we consider skin tone as the sensitive attribute. As with the CelebA dataset, we use ITA as a proxy for skin tone, with S a binary variable that denotes whether or not the ITA of the fundus is ≤ 19 , denoting that the individual has dark skin, as done by [12]. This has the advantage of being significantly easier to determine compared to the expensive and time consuming process of having a clinician manually annotate images. We compare these results with additional experiments we run using a smaller partition of the dataset with the race labels manually added by a ophthalmologist as done in [67], determined based on factors that might correlate with race such as the darkness of pigmentation in the fundus, thickness of blood vessels, and ratio of the optic cup size to optic disk size.

D. Experiment Details and Results

We perform experiments on the EyePACS, CelebA, and FairFace datasets, considering the challenging case of severe

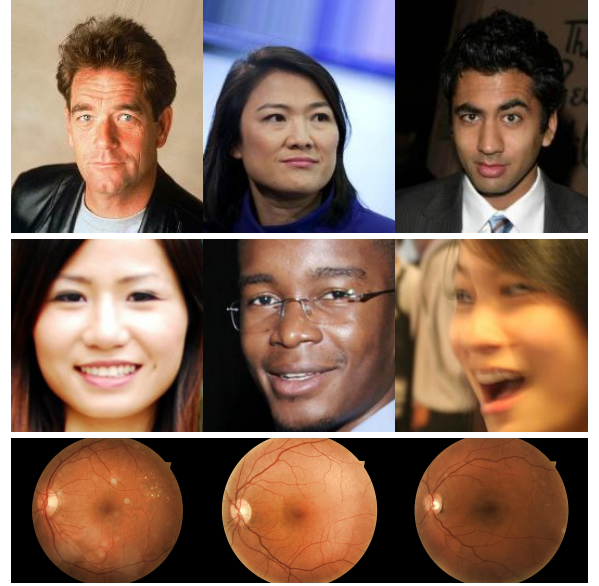


Fig. 2. Examples of images taken respectively from CelebA (top row), FairFace (middle row), and EyePACS (bottom row) datasets. For the EyePACS images, for the left image $(Y, S) = (1, 0)$, for the middle $(Y, S) = (0, 0)$, and for the right $(Y, S) = (0, 1)$.

data imbalance where training data is completely missing for one protected subgroup (e.g., diseased dark skin individuals for EyePACS).

1) *Hyper-parameter Tuning*: For all datasets, we conduct a hyper-parameter sweep, using various combinations of hyper-parameters β_1 and β_2 varied linearly from 1 to 50 and α varied linearly from 0 to 1, where $\alpha = 1$ signifies KL divergence instead of Rényi divergence. While we mostly focus on values of $\alpha < 1$, as these correspond to an approximation of a tighter upper bound that we expect would lead to better results, we also run several experiments with values of $\alpha > 1$.

As our RFIB method subsumes IB and CFB, with each of their hyper-parameters corresponding to one of RFIB’s hyper-parameters, we compare RFIB with those two methods. Setting $\alpha = 1$ and $\beta_1 = 0$ or $\beta_2 = 0$ results in RFIB being equivalent to CFB or IB, respectively, as the latter two systems are based on KL divergence and only have a single β hyper-parameter. We do separate comparisons of CFB, IB with RFIB, picking a commonly used value that performs well for CFB, IB and setting RFIB’s corresponding hyperparameter to the same value. We then use grid search to tune the two additional hyper-parameters that our method introduces; to compare with IB we fix a value of β_1 and tune α and β_2 , while to compare with CFB we fix a value of β_2 and then tune α and β_1 .

We implement the IB and CFB methods ourselves and also compare RFIB with two methods used by [12]: adversarial independence, referred to as adversarial debiasing (AD), that minimizes conditional dependence of predictions on sensitive attributes with an adversarial two player game and intelligent augmentation (IA) that generates synthetic data for under-represented populations and performs data augmentation to train a less biased model. To compare with AD and IA, we take results from [12] and report their original CAI scores

calculated with respect to their baseline, while for IB and CFB we implement the methods ourselves and calculate CAI scores with respect to results from our own baseline, a ResNet50 network [59].

We recapitulate most acronyms used in Table I.

TABLE I
LIST OF ACRONYMS USED.

| Acronym | Stands for |
|---------|---|
| AD | Adversarial Debiasing |
| CAI | Conjunctive Accuracy Improvement |
| CFB | Conditional Fairness Bottleneck |
| DR | Diabetic Retinopathy |
| IA | Intelligent Augmentation |
| IB | Information Bottleneck |
| ITA | Individual Topology Angle |
| KL | Kullback-Leibler |
| RFIB | Rényi Fair Information Bottleneck |
| UMAP | Uniform Manifold Approximation and Projection |

2) *EyePACS Results*: We predict $Y = \text{DR}$ status while using $S = \text{ITA}$ as the sensitive attribute. We consider a scenario where training data is completely missing for the subgroup of $(Y, S) = (1, 1)$, individuals referable for DR who have dark skin. The goal of our method is for predictions on the missing subgroup to be just as accurate as on the group with adequate training data, which is a problem of both fairness and also *domain adaptation*, achieving high performance on a group not present in the original dataset. This scenario matches an important real world problem where data for a minority subgroup such as dark skinned individuals is lacking.

We create a training partition containing both images referable and non-referable for DR of light skin individuals but only non-referable images of dark skin individuals. We use the same partition as in [12] to compare with their method, using a training set that consists of 10,346 light skin images referable for diabetic retinopathy ($\text{DR} = 1, \text{ITA} = 0$), 5,173 non-referable light skin images ($\text{DR} = 0, \text{ITA} = 0$), and 5,173 non-referable dark skin images ($\text{DR} = 0, \text{ITA} = 1$). Then for a fair assessment of our method’s performance we evaluate on a balanced test set with an equal number of positive and negative examples for both dark and light skin individuals, with the set containing 2,400 images equally balanced across DR and ITA.

As shown in Table II, our method outperforms all other methods, showing improvements in accuracy and fairness across all metrics. We show a result with a value of $\alpha > 1$ in the bottom row, showing that it is still possible to achieve promising performance with higher α values, although best results for most metrics were achieved with values of $\alpha < 1$, as expected since these values correspond to an approximation of a tighter upper bound on the $I(Z; X)$ mutual information term (that is being minimized). Usual caution should be exercised in interpretations since – despite our aligning with data partitioning in [12] – other variations may exist with [12], [38], [54] due to non-determinism, parameter setting or other factors.

We perform a second experiment where we use the same networks from before trained using $S = \text{ITA}$ but test on a

balanced test set where $S = \text{Ethnicity}$ (defined as in [12]), with labels coming from a human clinician. The test set consists of 400 images equally balanced across DR and ethnicity. We show these experimental results in Table III, where we outperform the other methods across most metrics, including the most important CAI scores. As we achieve similar results using ITA and race labels from a human clinician, we show that ITA can successfully be used as an easily obtained alternative to manual label annotation, further supporting conclusions reached by [12]. These results also demonstrate the ability of our method to perform well in this type of protected factor domain adaptation problem where a different protected factor is used after initial training, which is important in settings where the actual protected factor is not revealed for privacy reasons.

3) *CelebA Results*: We predict age using ITA as the sensitive attribute. Again, we consider the domain adaptation/fairness problem where part of the data is completely missing for a protected subgroup. In this case, older light skin images are missing and we use a training set of 48,000 images, consisting of 24,000 older dark skin images, 12,000 younger light skin images, and 12,000 older dark skin images. We use a test set of 8,000 images equally balanced across age and ITA, using the same partition as [12] and varying hyperparameters and comparing methods the same way as for EyePACS. Our results are shown in Table IV, showing our method performs the best across all metrics.

4) *FairFace Results*: We predict $Y = \text{Gender}$ with $S = \text{Race}$ as the sensitive attribute, testing on a test set balanced across gender and race. As before, we exclude one population subgroup and remove Black females from the training data, matching the common real-world scenario where data is lacking for this group. Unlike the previous experiments, here we can obtain race directly from the dataset rather than using ITA as a proxy for skin tone. We binarize the race labels into two groups, a smaller Black group and a larger non-Black group. We use a training set of 16,500 images, consisting of 5,500 male Black images, 5,500 male white images, and 5,500 female white images. We test on a test set of 3,000 images equally balanced across gender and race. Our results, given in Table V, show that we outperform both the IB and CFB methods both on accuracy and on all fairness metrics.

E. UMAP Clustering Analysis and Influence of α

We use UMAP [68] to provide a visual illustration of the effect of α . In Fig. 3, we show 2-dimensional UMAP vectors of our representation Z , coloring the points both based on the label Y and sensitive attribute S . Here experiments were done on the EyePACS dataset with $Y = \text{DR}$ and $S = \text{ITA}$. The goal is for the representation to preserve information about Y , allowing the two classes of Y to be easily separated, while removing the sensitive information S and preventing its two classes from being distinguished.

A value of $\alpha = 0$ corresponds to no compression with $I(Z; X) = 0$, which preserves maximum accuracy but does not help fairness, with the classes of both Y and S being easily separated as shown in Fig. 3. Increasing α gradually results in

TABLE II

RESULTS FOR DEBIASING METHODS ON EYEPACS PREDICTING $Y = \text{DR STATUS}$, TRAINED ON PARTITIONING WITH RESPECT TO $S = \text{ITA}$, AND EVALUATED ON A TEST SET BALANCED ACROSS DR STATUS AND ITA. FOR METRICS WITH AN \uparrow HIGHER IS BETTER WHEREAS FOR \downarrow LOWER IS BETTER. SUBPOPULATION IS THE ONE THAT CORRESPONDS TO THE MINIMUM ACCURACY, WITH (D) INDICATING DARK SKIN AND (L) LIGHT SKIN. METRICS ARE GIVEN AS PERCENTAGES.

| Methods | $acc \uparrow$ | $acc_{gap} \downarrow$ | $acc_{min} \uparrow$ (subpop.) | $CAI_{0.5} \uparrow$ | $CAI_{0.75} \uparrow$ | $dp_{gap} \downarrow$ | $eqodds_{gap} \downarrow$ |
|---|----------------|------------------------|-----------------------------------|----------------------|-----------------------|-----------------------|---------------------------|
| Baseline (from [12]) | 70.0 | 3.5 | 68.3 | - | - | NA | NA |
| AD ($\beta = 0.5$) ([12]) | 76.12 | 2.41 | 74.92 (L) | 3.61 | 2.35 | NA | NA |
| IA ([12]) | 71.5 | 1.5 | 70.16 (D) | 1.75 | 1.875 | NA | NA |
| Baseline (ours) | 73.37 | 8.08 | 69.33 (D) | - | - | 28.25 | 36.33 |
| IB ($\beta_1=30$) ([54]) | 74.12 | 2.08 | 73.08 (D) | 3.37 | 4.69 | 18.58 | 20.67 |
| CFB ($\beta_2=30$) ([38]) | 77.83 | 1.66 | 77.0 (L) | 5.44 | 5.93 | 10.83 | 12.5 |
| RFIB (ours) ($\alpha = 0.8, \beta_1 = 36, \beta_2 = 30$) | 79.42 | 0.5 | 79.17 (L) | 6.81 | 7.19 | 16.17 | 16.67 |
| RFIB (ours) ($\alpha = 0.3, \beta_1 = 30, \beta_2 = 50$) | 79.71 | 1.75 | 78.83 (L) | 6.33 | 6.33 | 9.75 | 11.50 |
| RFIB (ours) ($\alpha = 1.8, \beta_1 = 30, \beta_2 = 17$) | 78.35 | 0.25 | 78.25 (L) | 6.41 | 7.12 | 15.58 | 15.83 |

TABLE III

PERFORMANCE RESULTS FOR DEBIASING METHODS ON EYEPACS PREDICTING $Y = \text{DR STATUS}$, TRAINED ON PARTITIONING WITH RESPECT TO $S = \text{ITA}$, AND EVALUATED ON A TEST SET BALANCED ACROSS DR STATUS AND ETHNICITY (DEFINED AS IN [35]). FOR METRICS WITH AN \uparrow HIGHER IS BETTER WHEREAS FOR \downarrow LOWER IS BETTER. SUBPOPULATION IS THE ONE THAT CORRESPONDS TO THE MINIMUM ACCURACY, WITH (W) INDICATING WHITE INDIVIDUALS AND (B) BLACK INDIVIDUALS. METRICS ARE GIVEN AS PERCENTAGES.

| Methods | $acc \uparrow$ | $acc_{gap} \downarrow$ | $acc_{min} \uparrow$ (subpop.) | $CAI_{0.5} \uparrow$ | $CAI_{0.75} \uparrow$ | $dp_{gap} \downarrow$ | $eqodds_{gap} \downarrow$ |
|---|----------------|------------------------|-----------------------------------|----------------------|-----------------------|-----------------------|---------------------------|
| Baseline | 76.00 | 13.00 | 69.50 (B) | - | - | 3.00 | 16.00 |
| IB ($\beta_2=30$) ([38]) | 78.75 | 3.50 | 77.00 (B) | 6.12 | 7.81 | 0.50 | 4.00 |
| CFB ($\beta_2=30$) ([38]) | 75.00 | 6.00 | 72.00 (B) | 3.00 | 5.00 | 5.00 | 11.00 |
| RFIB (ours) ($\alpha = 0.8, \beta_1 = 36, \beta_2 = 30$) | 81.5 | 6.00 | 78.50 (B) | 6.25 | 6.63 | 3.00 | 9.00 |
| RFIB (ours) ($\alpha = 0.3, \beta_1 = 30, \beta_2 = 50$) | 81.75 | 4.50 | 79.50 (B) | 7.13 | 7.81 | 11.50 | 16.00 |

the different points getting more mixed together. While this is seen for both Y and S , the $I(Z; Y)$ and $I(Z; Y|S)$ terms help ensure that information about Y is still preserved, allowing the classes of Y to still separate fairly well even with higher compression, whereas the classes of S get mixed together as desired.

We note that an intermediate value of α can potentially provide the best compromise between fairness and accuracy, as a more moderate amount of compression can be enough to sufficiently remove sensitive information and further compression might only harm accuracy. This is illustrated in Fig. 3 where a value of $\alpha = 0.5$ was sufficient to mix together the classes of S while still preserving an obvious separation of the two classes of Y . Further increasing α worsened the separation of Y more than it added additional benefit for S . This is also supported by our experimental results where best overall accuracy-fairness trade-offs were typically obtained for intermediate values of α .

V. CONCLUSION

We propose RFIB, a novel variational IB method based on Rényi divergence that offers trade-offs in utility, two fairness objectives, and compactness. Using Rényi divergence instead of KL divergence gives a way to control the amount of compression with an additional hyper-parameter. Compared to prior work which incorporates a single definition of fairness, RFIB has the potential benefit of allowing ethicists and policy

makers to specify softer and more balanced requirements for fairness that lie between multiple hard requirements, and our work opens the way to future studies expanding on this idea. Experimental results on three different image datasets showed RFIB provides benefits vis-a-vis other methods of record including IB, CFB, and other techniques performing augmentation or adversarial debiasing.

REFERENCES

- [1] A. Gronowski, W. Paul, F. Alajaji, B. Ghahesifard, and P. Burlina, “Rényi fair information bottleneck for image classification,” in *Proc. 17th Canadian Workshop on Information Theory*, June 2022, pp. 1 – 5. [Online]. Available: <http://cwit.ca/2022/papers/1570796577.pdf>
- [2] N. M. Kinyanjui, T. Odonga, C. Cintas, N. C. Codella, R. Panda, P. Sattigeri, and K. R. Varshney, “Fairness of classifiers across skin tones in dermatology,” in *International Conference on Medical Image Computing and Computer-Assisted Intervention*, 2020, pp. 320–329.
- [3] T. Bolukbasi, K.-W. Chang, J. Y. Zou, V. Saligrama, and A. T. Kalai, “Man is to computer programmer as woman is to homemaker? Debiasing word embeddings,” in *Proc. Adv. Neural Inform. Process. Syst.*, 2016, pp. 4349–4357.
- [4] R. Zemel, Y. Wu, K. Swersky, T. Pitassi, and C. Dwork, “Learning fair representations,” in *Proc. Int. Conf. Mach. Learn.*, 2013, pp. 325–333.
- [5] F. Prost, H. Qian, Q. Chen, E. H. Chi, J. Chen, and A. Beutel, “Toward a better trade-off between performance and fairness with kernel-based distribution matching,” *arXiv:1910.11779*, 2019.
- [6] S. Caton and C. Haas, “Fairness in machine learning: A survey,” *arXiv:2010.04053*, 2020.
- [7] N. Tishby, F. C. Pereira, and W. Bialek, “The information bottleneck method,” in *Proceedings of the 37th Annual Allerton Conference on Communication, Control, and Computing*, 1999, p. 368–377.

TABLE IV

RESULTS FOR DEBIASING METHODS ON CELEBA PREDICTING $Y = \text{AGE}$, TRAINED ON PARTITIONING WITH RESPECT TO $S = \text{ITA}$, AND EVALUATED ON A TEST SET BALANCED ACROSS AGE AND ITA. FOR METRICS WITH AN \uparrow HIGHER IS BETTER WHEREAS FOR \downarrow LOWER IS BETTER. SUBPOPULATION IS THE ONE THAT CORRESPONDS TO THE MINIMUM ACCURACY, WITH (D) INDICATING DARK SKIN AND (L) LIGHT SKIN. METRICS ARE GIVEN AS PERCENTAGES.

| Methods | $acc \uparrow$ | $acc_{gap} \downarrow$ | $acc_{min} \uparrow$ (subpop.) | $CAI_{0.5} \uparrow$ | $CAI_{0.75} \uparrow$ | $dp_{gap} \downarrow$ | $eqodds_{gap} \downarrow$ |
|---|----------------|------------------------|-----------------------------------|----------------------|-----------------------|-----------------------|---------------------------|
| Baseline (from [12]) | 74.4 | 13.9 | 67.5 | - | - | NA | NA |
| AD ($\beta = 0.5$) ([12]) | 76.45 | 9.6 | 71.65 (D) | 3.17 | 3.75 | NA | NA |
| IA ([12]) | 75.29 | 9.18 | 70.7 (D) | 2.8 | 1.56 | NA | NA |
| Baseline (ours) | 70.61 | 16.57 | 62.32 (D) | - | - | 43.82 | 60.4 |
| IB ($\beta_1=30$) ([54]) | 71.76 | 14.87 | 64.32 (D) | 1.42 | 4.69 | 36.62 | 51.5 |
| CFB ($\beta_2=30$) ([38]) | 71.77 | 13.25 | 65.15 (D) | 2.24 | 2.78 | 38.3 | 51.55 |
| RFIB (ours) ($\alpha = 0.3, \beta_1 = 30, \beta_2 = 43$) | 75.04 | 10.92 | 69.57 (D) | 5.04 | 5.34 | 29.02 | 39.95 |
| RFIB (ours) ($\alpha = 0.4, \beta_1 = 1, \beta_2 = 30$) | 76.92 | 5.05 | 74.4 (D) | 8.91 | 10.22 | 2.7 | 7.75 |

TABLE V

RESULTS FOR DEBIASING METHODS ON FAIRFACE PREDICTING $Y = \text{GENDER}$, TRAINED ON PARTITIONING WITH RESPECT TO $S = \text{RACE}$, AND EVALUATED ON A TEST SET BALANCED ACROSS GENDER AND ITA. FOR METRICS WITH AN \uparrow HIGHER IS BETTER WHEREAS FOR \downarrow LOWER IS BETTER. SUBPOPULATION IS THE ONE THAT CORRESPONDS TO THE MINIMUM ACCURACY, WITH (B) INDICATING BLACK. METRICS ARE GIVEN AS PERCENTAGES.

| Methods | $acc \uparrow$ | $acc_{gap} \downarrow$ | $acc_{min} \uparrow$ (subpop.) | $CAI_{0.5} \uparrow$ | $CAI_{0.75} \uparrow$ | $dp_{gap} \downarrow$ | $eqodds_{gap} \downarrow$ |
|---|----------------|------------------------|-----------------------------------|----------------------|-----------------------|-----------------------|---------------------------|
| Baseline | 73.97 | 16.47 | 65.73 (B) | - | - | 27.53 | 44.0 |
| IB ($\beta_2=30$) ([54]) | 73.93 | 14.93 | 68.6 (B) | 0.75 | 1.14 | 30.0 | 44.93 |
| CFB ($\beta_2=30$) ([38]) | 75.6 | 14.0 | 65.2 (B) | 2.05 | 2.26 | 26.27 | 40.27 |
| RFIB (ours) ($\alpha = 0.2, \beta_1 = 30, \beta_2 = 29$) | 83.6 | 8.53 | 79.33 (B) | 8.78 | 8.36 | 19.47 | 28.0 |
| RFIB (ours) ($\alpha = 0.2, \beta_1 = 1, \beta_2 = 30$) | 82.07 | 7.33 | 78.4 (B) | 8.62 | 8.88 | 19.07 | 26.4 |

- [8] M. Hardt, E. Price, and N. Srebro, "Equality of opportunity in supervised learning," in *Proc. Adv. Neural Inform. Process. Syst.*, 2016, pp. 3315–3323.
- [9] G. Pleiss, M. Raghavan, F. Wu, J. Kleinberg, and K. Q. Weinberger, "On fairness and calibration," in *Proc. Adv. Neural Inform. Process. Syst.*, 2017, pp. 5680–5689.
- [10] T. Karras, S. Laine, and T. Aila, "A style-based generator architecture for generative adversarial networks," in *Proc. IEEE Conf. Comput. Vis. Pattern Recog.*, 2019, pp. 4401–4410.
- [11] A. Grover, J. Song, A. Kapoor, K. Tran, A. Agarwal, E. J. Horvitz, and S. Ermon, "Bias correction of learned generative models using likelihood-free importance weighting," in *Proc. Adv. Neural Inform. Process. Syst.*, 2019, pp. 11 058–11 070.
- [12] W. Paul, A. Hadzic, N. Joshi, F. Alajaji, and P. Burlina, "TARA: Training and representation alteration for AI fairness and domain generalization," *Neural Computation*, vol. 34, no. 3, pp. 716–753, 2022.
- [13] N. Quadrianto, V. Sharmanska, and O. Thomas, "Discovering fair representations in the data domain," in *Proc. IEEE Conf. Comput. Vis. Pattern Recog.*, 2019, pp. 8227–8236.
- [14] S. Hwang, S. Park, D. Kim, M. Do, and H. Byun, "Fairfacegan: Fairness-aware facial image-to-image translation," in *Proc. Brit. Mach. Vis. Conf.*, 2020.
- [15] P. Sattigeri, S. C. Hoffman, V. Chenthamarakshan, and K. R. Varshney, "Fairness GAN: Generating datasets with fairness properties using a generative adversarial network," *IBM Journal of Research and Development*, vol. 63, no. 4/5, pp. 3:1–3:9, 2019.
- [16] T. Karras, S. Laine, M. Aittala, J. Hellsten, J. Lehtinen, and T. Aila, "Analyzing and improving the image quality of StyleGAN," in *Proc. IEEE Conf. Comput. Vis. Pattern Recog.*, 2020.
- [17] C. Wadsworth, F. Vera, and C. Piech, "Achieving fairness through adversarial learning: an application to recidivism prediction," in *Conference on Fairness, Accountability, and Transparency in Machine Learning (FATML)*, 2018.
- [18] B. H. Zhang, B. Lemoine, and M. Mitchell, "Mitigating unwanted biases with adversarial learning," in *Proceedings of the 2018 AAAI/ACM Conference on AI, Ethics, and Society*, 2018, pp. 335–340.
- [19] H. Edwards and A. Storkey, "Censoring representations with an adversary," in *Proc. Int. Conf. Learn. Represent.*, 2016.
- [20] A. Beutel, J. Chen, Z. Zhao, and E. H. Chi, "Data decisions and theoretical implications when adversarially learning fair representations," *arXiv:1707.00075*, 2017.
- [21] D. Madras, E. Creager, T. Pitassi, and R. Zemel, "Learning adversarially fair and transferable representations," in *Proc. Int. Conf. Mach. Learn.*, 2018, pp. 3384–3393.
- [22] P. C. Roy and V. N. Boddeti, "Mitigating information leakage in image representations: A maximum entropy approach," in *Proc. IEEE Conf. Comput. Vis. Pattern Recog.*, 2019, pp. 2586–2594.
- [23] H. Zhao, A. Coston, T. Adel, and G. J. Gordon, "Conditional learning of fair representations," in *Proc. Int. Conf. Learn. Represent.*, 2020.
- [24] S. Pföhl, B. Marafino, A. Coulet, F. Rodriguez, L. Palaniappan, and N. H. Shah, "Creating fair models of atherosclerotic cardiovascular disease risk," in *Proceedings of the 2019 AAAI/ACM Conference on AI, Ethics, and Society*, 2019, pp. 271–278.
- [25] X. Gitiaux and H. Rangwala, "Learning smooth and fair representations," in *International Conference on Artificial Intelligence and Statistics*. PMLR, 2021, pp. 253–261.
- [26] V. Grari, S. Lamprier, and M. Detryniecki, "Fairness-aware neural Rényi minimization for continuous features," in *Proceedings of the Twenty-Ninth International Joint Conference on Artificial Intelligence*, ser. IJCAI'20, 2021.
- [27] J. Song, P. Kalluri, A. Grover, S. Zhao, and S. Ermon, "Learning controllable fair representations," in *Twenty-Second International Conference on Artificial Intelligence and Statistics*, 2019, pp. 2164–2173.
- [28] A. Kolchinsky, B. D. Tracey, and D. H. Wolpert, "Nonlinear information bottleneck," *Entropy*, vol. 21, no. 12, p. 1181, 2019.
- [29] I. Fischer, "The conditional entropy bottleneck," *Entropy*, vol. 22, no. 9, p. 999, 2020.
- [30] A. Makhdoumi, S. Salamatian, N. Fawaz, and M. Médard, "From the information bottleneck to the privacy funnel," in *2014 IEEE Information Theory Workshop (ITW 2014)*, 2014, pp. 501–505.
- [31] D. Strouse and D. J. Schwab, "The deterministic information bottleneck," *Neural computation*, vol. 29, no. 6, pp. 1611–1630, 2017.
- [32] H. Hsu, S. Asodeh, S. Salamatian, and F. P. Calmon, "Generalizing bottleneck problems," in *Proceedings of the IEEE International Symposium on Information Theory (ISIT)*, 2018, pp. 531–535.

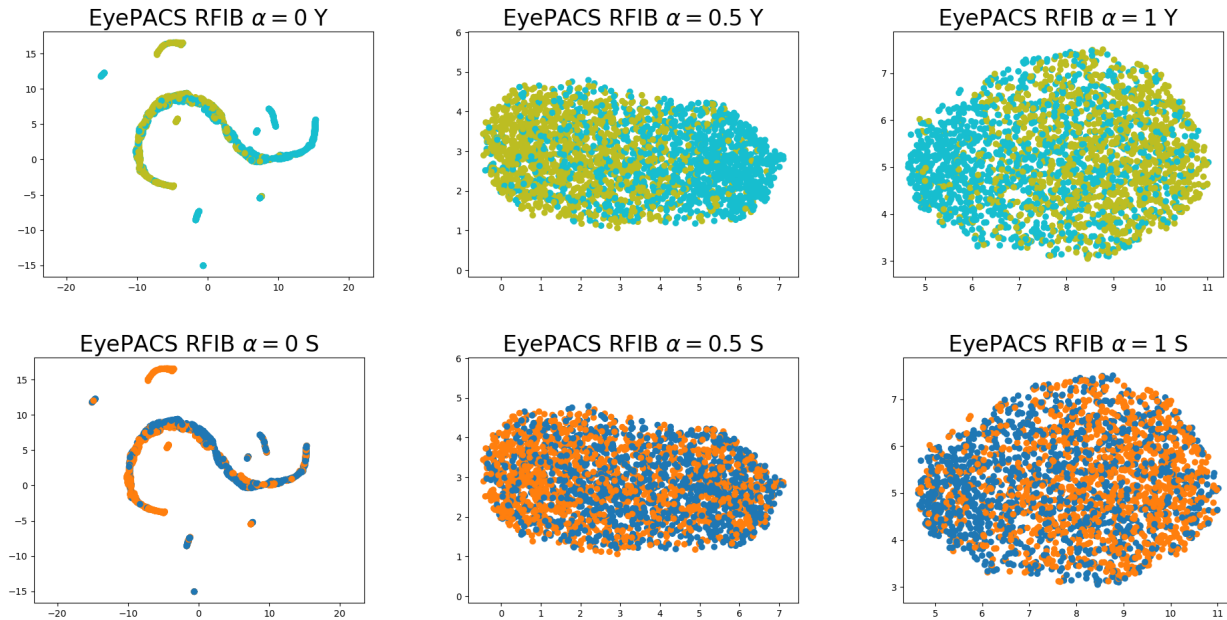


Fig. 3. UMAP dimensionality reduction of Z for the EyePACS dataset. The top row shows the two classes of Y (light blue representing the positive examples and light green the negative) while the bottom row shows the two classes of S (orange representing the positive examples and blue the negative). Going from left to right α is increased, resulting in more compression and causing a decrease in separation of the two classes. While separation occurs for both Y and S , it occurs to a greater extent for S as desired.

- [33] S. Asodeh and F. P. Calmon, "Bottleneck problems: An information and estimation-theoretic view," *Entropy*, vol. 22, no. 11, p. 1325, 2020.
- [34] J.-J. Weng, F. Alajaji, and T. Linder, "An information bottleneck problem with Rényi's entropy," in *Proceedings of the IEEE International Symposium on Information Theory (ISIT)*, 2021, pp. 2489–2494.
- [35] Z. Goldfeld and Y. Polyanskiy, "The information bottleneck problem and its applications in machine learning," *IEEE Journal on Selected Areas in Information Theory*, vol. 1, no. 1, pp. 19–38, 2020.
- [36] A. Zaidi, I. Estella-Aguerrí, and S. Shamai (Shitz), "On the information bottleneck problems: Models, connections, applications and information theoretic views," *Entropy*, vol. 22, no. 2, p. 151, 2020.
- [37] A. Ghassami, S. Khodadadian, and N. Kiyavash, "Fairness in supervised learning: An information theoretic approach," in *Proceedings of the IEEE International Symposium on Information Theory (ISIT)*, 2018, pp. 176–180.
- [38] B. Rodríguez-Gálvez, R. Thobaben, and M. Skoglund, "A variational approach to privacy and fairness," in *Proceedings of the IEEE Information Theory Workshop (ITW)*, 2021, pp. 1–6.
- [39] A. R. Esposito, M. Gastpar, and I. Issa, "Robust generalization via α -mutual information," in *Proceedings of the International Zurich Seminar on Information and Communication*, 2020, pp. 96–100.
- [40] Y. Li and R. E. Turner, "Rényi divergence variational inference," in *Proc. Adv. Neural Inform. Process. Syst.*, vol. 29, 2016, pp. 1073–1081.
- [41] I. Mironov, "Rényi differential privacy," in *IEEE 30th Computer Security Foundations Symposium (CSF)*, 2017, pp. 263–275.
- [42] H. Bhatia, W. Paul, F. Alajaji, B. Gharesifard, and P. Burlina, "Least k th-order and Rényi generative adversarial networks," *Neural Computation*, vol. 33, no. 9, pp. 2473–2510, 2021.
- [43] A. Sarraf and Y. Nie, "RGAN: Rényi generative adversarial network," *SN Computer Science*, vol. 2, no. 1, p. 17, 2021.
- [44] Y. Pantazis, D. Paul, M. Fasoulakis, Y. Stylianou, and M. A. Katsoulakis, "Cumulant GAN," *IEEE Transactions on Neural Networks and Learning Systems*, 2022.
- [45] G. R. Kurri, T. Sypherd, and L. Sankar, "Realizing GANs via a tunable loss function," in *Proceedings of the IEEE Information Theory Workshop (ITW)*, 2021, pp. 1–6.
- [46] S. Baharlouei, M. Nouched, A. Beirami, and M. Razaviyayn, "Rényi fair inference," in *Proc. Int. Conf. Learn. Represent.*, 2020.
- [47] S. Ben-David, J. Blitzer, K. Crammer, A. Kulesza, F. Pereira, and J. W. Vaughan, "A theory of learning from different domains," *Machine Learning*, vol. 79, no. 1, pp. 151–175, 2010.
- [48] Y. Ganin, E. Ustinova, H. Ajakan, P. Germain, H. Larochelle, F. Laviolette, M. Marchand, and V. Lempitsky, "Domain-adversarial training of neural networks," *The Journal of Machine Learning Research*, vol. 17, no. 1, pp. 2096–2030, 2016.
- [49] M. Long, Y. Cao, J. Wang, and M. Jordan, "Learning transferable features with deep adaptation networks," in *Proc. Int. Conf. Mach. Learn.*, 2015, pp. 97–105.
- [50] N. Zhang, M. Mohri, and J. Hoffman, "Multiple-source adaptation theory and algorithms," *Annals of Mathematics and Artificial Intelligence*, vol. 89, no. 3, pp. 237–270, 2021.
- [51] S. Sagawa, P. W. Koh, T. B. Hashimoto, and P. Liang, "Distributionally robust neural networks for group shifts: On the importance of regularization for worst-case generalization," in *Proc. Int. Conf. Mach. Learn.*, 2020.
- [52] N. Sohoni, J. Dunnmon, G. Angus, A. Gu, and C. Ré, "No subclass left behind: Fine-grained robustness in coarse-grained classification problems," *Proc. Adv. Neural Inform. Process. Syst.*, vol. 33, pp. 19 339–19 352, 2020.
- [53] T. Zhang, T. Zhu, K. Gao, W. Zhou, and S. Y. Philip, "Balancing learning model privacy, fairness, and accuracy with early stopping criteria," *IEEE Transactions on Neural Networks and Learning Systems*, 2021.
- [54] A. A. Alemi, I. Fischer, J. V. Dillon, and K. Murphy, "Deep variational information bottleneck," in *Proc. Int. Conf. Learn. Represent.*, 2017, pp. 1–17.
- [55] T. van Erwen and P. Harremoës, "Rényi divergence and Kullback-Leibler divergence," *IEEE Transactions on Information Theory*, vol. 60, no. 7, pp. 3797 – 3820, 2014.
- [56] D. P. Kingma and M. Welling, "Auto-encoding variational Bayes," in *Proc. Int. Conf. Learn. Represent.*, 2014.
- [57] M. Gil, F. Alajaji, and T. Linder, "Rényi divergence measures for commonly used univariate continuous distributions," *Information Sciences*, vol. 249, pp. 124–131, 2013.
- [58] J. Burbea, "The convexity with respect to Gaussian distributions of divergences of order α ," *Utilitas Mathematica*, vol. 26, pp. 171–192, 1984.
- [59] K. He, X. Zhang, S. Ren, and J. Sun, "Deep residual learning for image recognition," in *Proceedings of the IEEE Conference on Computer Vision and Pattern Recognition (CVPR)*, June 2016.
- [60] J. Rawls, *Justice as fairness: A restatement*. Harvard University Press, 2001.
- [61] Z. Liu, P. Luo, X. Wang, and X. Tang, "Deep learning face attributes in the wild," in *Proc. Int. Conf. Comput. Vis.*, December 2015.

- [62] M. Wilkes, C. Y. Wright, J. L. du Plessis, and A. Reeder, "Fitzpatrick skin type, individual typology angle, and melanin index in an african population: steps toward universally applicable skin photosensitivity assessments," *JAMA dermatology*, vol. 151, no. 8, pp. 902–903, 2015.
- [63] M. Merler, N. Ratha, R. S. Feris, and J. R. Smith, "Diversity in faces," *arXiv:1901.10436*, 2019.
- [64] N. M. Kinyanjui, T. Odonga, C. Cintas, N. C. Codella, R. Panda, P. Sattigeri, and K. R. Varshney, "Estimating skin tone and effects on classification performance in dermatology datasets," in *NeurIPS 2019 Workshop on Fair ML for Health*, 2019.
- [65] K. Karkkainen and J. Joo, "Fairface: Face attribute dataset for balanced race, gender, and age for bias measurement and mitigation," in *Proceedings of the IEEE/CVF Winter Conference on Applications of Computer Vision*, 2021, pp. 1548–1558.
- [66] EyePACS, "Diabetic retinopathy detection," Data retrieved from Kaggle, <https://www.kaggle.com/agaldran/eyepacs>, 2015.
- [67] P. Burlina, N. Joshi, W. Paul, K. D. Pacheco, and N. M. Bressler, "Addressing artificial intelligence bias in retinal disease diagnostics," *Translational Vision Science and Technology*, 2020.
- [68] L. McInnes, J. Healy, N. Saul, and L. Großberger, "UMAP: Uniform manifold approximation and projection," *Journal of Open Source Software*, vol. 3, no. 29, p. 861, 2018.